Journal of Applied Physics

RESEARCH ARTICLE | OCTOBER 21 2022

Effect of hydrogen on the unintentional doping of 4H silicon carbide

Yuanchao Huang ; Rong Wang ; Naifu Zhang ; Yiqiang Zhang; Deren Yang ; Xiaodong Pi

J. Appl. Phys. 132, 155704 (2022)
https://doi.org/10.1063/5.0108726

AIP Publishing

Journal of Applied Physics ARTICLE scitation.org/journal/jap

Effect of hydrogen on the unintentional doping of 4H silicon carbide

Cite as: J. Appl. Phys. **132**, 155704 (2022); doi: 10.1063/5.0108726
Submitted: 10 July 2022 · Accepted: 22 September 2022 ·
Published Online: 21 October 2022

Yuanchao Huang,[1,2] Rong Wang,[1,2] Naifu Zhang,[1,2] Yiqiang Zhang,[3] Deren Yang,[1,2] and Xiaodong Pi[1,2,a)]

AFFILIATIONS

[1]State Key Laboratory of Silicon Materials and School of Materials Science and Engineering, Zhejiang University, Hangzhou, Zhejiang 310027, China
[2]Institute of Advanced Semiconductors and Zhejiang Provincial Key Laboratory of Power Semiconductor Materials and Devices, Hangzhou Innovation Center, Zhejiang University, Hangzhou, Zhejiang 310027, China
[3]School of Materials Science and Engineering and College of Chemistry, Zhengzhou University, Zhengzhou, Henan 450001, China

[a)]**Author to whom correspondence should be addressed:** xdpi@zju.edu.cn

ABSTRACT

High-purity semi-insulating (HPSI) 4H silicon carbide (4H-SiC) single crystals are critical semiconductor materials for fabricating GaN-based high-frequency devices. One of the major challenges for the growth of HPSI 4H-SiC single crystals is the unintentional doping of nitrogen (N) and boron (B). The addition of hydrogen has been supposed to mitigate unintentional doping. However, the underlying mechanism has not been well understood. In this work, the role of hydrogen in the growth of HPSI 4H-SiC single crystals is investigated by first-principles formation-energy calculations. We find that the addition of hydrogen significantly mitigates N doping while hardly affecting B doping. Once hydrogen is added, hydrogen may adsorb at the growing surface of 4H-SiC, leading to surface passivation. Since N can react with hydrogen to form stable NH_3 (g), the chemical potential of N is reduced, so that the formation energy of N in 4H-SiC increases. Hence, the critical partial pressure of nitrogen required for the growth of HPSI 4H-SiC single crystals increases by two orders of magnitude. Moreover, we reveal that the adjustment of relative B and N doping concentrations has a substantial impact on the Fermi energy of HPSI 4H-SiC. When the doping concentration of N is higher than that of B, N interacts with carbon vacancies (V_C) to pin the Fermi energy at $Z_{1/2}$. When the doping concentration of B is higher than that of N, the Fermi energy is pinned at EH6/7. This explains that the resistivity of unintentionally doped HPSI 4H-SiC may vary.

I. INTRODUCTION

High-purity semi-insulating (HPSI) 4H silicon carbide (4H-SiC) single crystals are now routinely processed to make wafers that are substrates for GaN-based high-frequency devices due to the superior physical properties such as wide bandgap, high resistivity, high thermal conductivity, and strong breakdown field of HPSI 4H-SiC.[1–6] In order to achieve the high resistivity (>10^5 Ω cm), shallow donors and acceptors in 4H-SiC must be compensated or avoided. Two general approaches may be used to compensate shallow donors and acceptors. One is intentional doping of vanadium (V).[7,8] The other is creation of intrinsic defects in 4H-SiC.[9–17] Doping of V may lead to deterioration of crystal quality and low processing yield.[7,8] Thus, intrinsic defects produced by a series of methods such as irradiation are more often used to compensate shallow donors and acceptors.[9] It is clear that shallow donors and acceptors are most preferably avoided during growth of 4H-SiC for the sake of high resistivity. Nitrogen (N) and boron (B) are considered major dopants that may be readily doped without intention because N and B exist in graphite parts and source powders used in a 4H-SiC growth system.[10–12]

Various approaches for avoiding unintentional doping of N and B have been investigated. For example, ultra-pure source powders and graphite parts with negligible N and B were employed to more efficiently remove N and B.[10,13] Higher vacuum was employed to more efficiently remove N. Inert gas was directly incorporated into the crystal-growth zone of 4H-SiC to eliminate N there.[10–19] Through these approaches, the doping concentration of

B in grown 4H-SiC can be decreased in an order of 10^{15} cm^{-3} and the lowest doping concentration of N is in an order of 10^{16}–10^{17} cm^{-3}. However, this doping level was insufficient to guarantee that the grown 4H-SiC has a uniform semi-insulating characteristic. It was claimed that the addition of hydrogen might reduce unintentional doping of N during the growth of 4H-SiC single crystals by physical vapor transport (PVT).[13,16,17] As a consequence, the N incorporation was remarkably reduced, leading to the growth of semi-insulating 4H-SiC single crystals. Regarding the underlying mechanism, it was proposed that hydrogen reacted with graphite to form hydrocarbons, increasing the C/Si ratio during growth of 4H-SiC.[18] Since N and C compete for the same lattice sites,[1] the increase in the C/Si ratio significantly reduced N doping of 4H-SiC. It was also argued that hydrogen passivated the surface of 4H-SiC, preventing nitrogen from occupying the surface sites during 4H-SiC growth.[16,17] Both explanations, however, are rather speculative. In this work, first-principle formation-energy calculations are carried out to reveal the effect of hydrogen on unintentional doping of 4H-SiC. It is found that hydrogen reacts with nitrogen to form stable ammonia (NH_3) at the growing surface of 4H-SiC. This leads to the decrease in the chemical potential of N, increasing the formation energy of N in 4H-SiC. Hence, HPSI 4H-SiC may be grown by using a relatively high partial pressure of nitrogen. Moreover, we find that the control of the relative concentrations of unintentionally doped B and N has a substantial impact on the Fermi energy of HPSI 4H-SiC. When the concentration of N is higher than that of B, N interacts with carbon vacancies (V_C) so that the Fermi energy is pinned at $Z_{1/2}$. When the concentration of B is higher than that of N, the Fermi energy is pinned at EH6/7.

II. COMPUTATIONAL METHODS

First-principles calculations are performed using the projector-augmented wave (PAW) method implanted in the Vienna ab-initio Simulation Package (VASP). The wave functions are expanded by using the plane-wave energy cutoff of 500 eV. The Perdew–Burke–Ernzerhof (PBE) functional with generalized gradient approximation (GGA) exchange correlation is employed to describe exchange-correlation interactions.[20] Brillouin-zone integrations are approximated by using special k-point sampling of the Monkhorst–Pack scheme with a k-point mesh of $2 \times 2 \times 2$. The supercell lattice and atomic coordinates are fully relaxed until the total energy per cell and the force on each atom are less than 1.0×10^{-6} eV and 0.01 eV/Å, respectively. The screened hybrid density functional of Heyd, Scuseria, and Ernzerhof (HSE06) is adopted to calculate the electronic properties of 4H-SiC. Defects are modeled in a $4 \times 4 \times 1$ supercell of 4H-SiC with 128 atoms. The calculated lattice parameters of 4H-SiC are a = 3.07 Å and c = 10.05 Å. The calculated bandgap energy of 4H-SiC is 3.23 eV, which agrees well with experimental results.[1]

The formation energy of a charge-neutral defect α is calculated by using[21,22]

$$\Delta H_f(\alpha, 0) = E_{tot}(\alpha, 0) - E_{tot}(\text{host}) + \sum n_i \mu_i, \quad (1)$$

where $E_{tot}(\alpha, 0)$ is the total energy of the host supercell containing the defect α, $E_{tot}(\text{host})$ is the total energy of the host supercell, n_i is the number of atoms removed from or added into the supercell, and μ_i is the chemical potential of constituent i referred to elemental solid or gas. If the defect α is in the charge of q, the formation energy can be expressed as

$$\Delta H_f(\alpha, q) = \Delta H_f(\alpha, 0) - q\varepsilon(0/q) + qE_F, \quad (2)$$

where $\varepsilon(0/q)$ are charge-state transition levels and E_F is the Fermi energy referred to the valence band maximum (VBM) of the host. To overcome the issue of finite supercell size, $\varepsilon(0/q)$ is calculated with the mixed k-point scheme by using

$$\varepsilon(0/q) = [\varepsilon_D^{\tau}(0) - \varepsilon_{VBM}^{\tau}(host)] + [E_{tot}(\alpha, q) - (E_{tot}(\alpha, 0) - q\varepsilon_D^{k}(0))]/(-q), \quad (3)$$

where $\varepsilon_D^{\tau}(0)$ and $\varepsilon_D^{k}(0)$ are the energies of the defect band at the Γ point and special k point (weight averaged), respectively;[21] $\varepsilon_{VBM}^{\tau}(host)$ is the VBM of the host at the Γ point; and $E_{tot}(\alpha, q)$ is the total energy of the host supercell containing defect α with charge q. For Eq. (3), the first term on the right-hand side gives the single-electron energy level of the defect at Γ point, while the second term on the right-hand side determines the relaxation energy U of the charged defect calculated at the special k point, which is the extra cost of energy by moving charge q from the VBM of the host to the defect level.

III. RESULTS AND DISCUSSIONS

Thermal equilibrium conditions exert a series of thermodynamic limits on the achievable values of μ_i. First, the values of μ_{Si} and μ_C are limited to those values that maintain stable 4H-SiC,

$$\mu_{Si} + \mu_C = \Delta H_f(\text{SiC}). \quad (4)$$

Second, for the avoidance of precipitation of Si, C, B, and N_2, the values of μ_i are limited by

$$\mu_{Si} \le 0, \mu_C \le 0, \mu_B \le 0, \mu_N \le 0. \quad (5)$$

Finally, the formation of the secondary phase needs to be avoided. In order to make the consideration of secondary compounds as complete as possible, the material genome database (Materials Project) is used to search for the competing secondary compounds.[23] Through the formation energy information of all the secondary compounds for Si–C–B and Si–C–N system, we find that the formation of SiB_3, $B_{39}C_6$, and Si_3N_4 limits the stable chemical potential region due to the lowest formation energy. The calculated formation energies and experimental values of 4H-SiC, SiB_3, $B_{39}C_6$, and Si_3N_4 are summarized in Table I. Hence, the values of μ_i are limited by

$$\mu_{Si} + 3\mu_B \le \Delta H_f(SiB_3),\ 39\mu_B + 6\mu_C \le \Delta H_f(B_{39}C_6),\ 4\mu_N + 3\mu_{Si} \le \Delta H_f(Si_3N_4), \quad (6)$$

where $\Delta H_f(SiB_3)$, $\Delta H_f(B_{39}C_6)$, and $\Delta H_f(Si_3N_4)$ are the formation

TABLE I. DFT-calculated formation energies and experimental values (Expt.) of 4H-SiC, SiB_3, $B_{39}C_6$, and Si_3N_4.

	DFT calculated ΔH_f	Expt. ΔH_f
4H-SiC	−0.7309 eV/SiC	−0.676, −0.747, or −0.771 eV/SiC[24]
SiB_3	−1.309 eV/SiB_3	−1.196 eV/SiB_3[25]
$B_{39}C_6$	−3.678 eV/$B_{39}C_6$	…
Si_3N_4	−8.323 eV/Si_3N_4	−7.7173 eV/Si_3N_4[26]

TABLE II. The accessible range for B and N chemical potential.

	Equilibrium state	Growth on C-face	Growth on C-face with hydrogen
Chemical potential of B	Region I	Region I and region II	Region I and region II
Chemical potential of N	Region I	Region I, region II, and region III	Region I and region II

energies of SiB_3, $B_{39}C_6$, and Si_3N_4, respectively. By solving Eqs. (4)–(6), we obtain the accessible range for μ_B and μ_N [region I in Figs. 1(a) and 1(b)].

As for B or N doping during the PVT growth of 4H-SiC, B or N is incorporated at the growing surface. Normally, 4H-SiC crystal grows on a SiC seed with the $(000\bar{1})$ face (i.e., C face), while 6H-SiC grows on a SiC seed with the (0001) face (i.e., Si face). The accessible range of μ_B or μ_N for B or N doping on the surface of SiC is larger than the equilibrium range [region I in Figs. 1(a) and 1(b)], consistent with previous findings that doping on the surface led to the increase in the chemical potential and solubility of the dopant.[27,28] This is because initial precipitation of the dopant on the growing surface costs more energy than doping in the bulk. We have considered the effect of C face on the chemical potential of B or N. A simple estimation for the upper limit of μ_B or μ_N under the conditions of PVT growth is made by considering the spontaneous accumulation of the dopant at the top surface layer: ΔH_f^{surf}(N or B, 0) = 0. For growth on the C face, the accessible range of μ_B expands to region I and region II [Fig. 1(a)]. The accessible range of μ_N expands to region I, region II, and region III [Fig. 1(b)]. Furthermore, hydrogen may affect the chemical potential range of μ_N. Once the hydrogen is added, hydrogen will adsorb to the growing surface and passivate it. When N

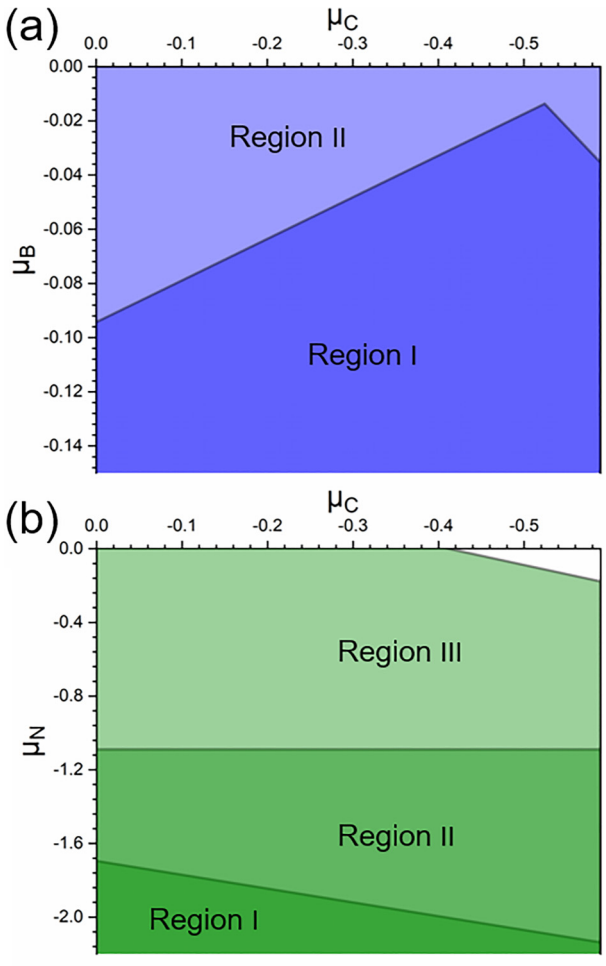

FIG. 1. (a) Accessible range of chemical potential of μ_B. (b) Accessible range of chemical potential of μ_N.

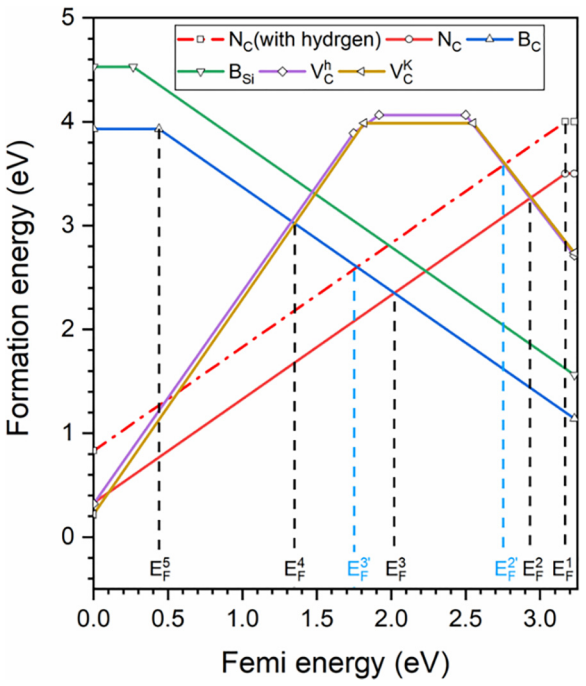

FIG. 2. Formation energies of B, N, and V_C at the Si-rich limit.

adsorbs to the growing surface, N may react with hydrogen to form stable NH_3 (g).[29] Therefore,

$$\mu_N + 3\mu_H = \Delta H_f(NH_3). \quad (7)$$

This restricts the accessible range of μ_N in region I and region II [Fig. 1(b)]. The accessible ranges of the chemical potentials of B and N under different conditions are summarized in Table II.

The effect of temperature and the partial pressure of N/B is further considered. $\mu_{N/B}$ can be given as[30]

$$\mu_{N/B} = \mu_{N/B}^{max} + RT\ln(P_{N/B}/P_0), \quad (8)$$

where $\mu_{N/B}^{max}$ is the max value of $\mu_{N/B}$, R is the molar gas constant, T

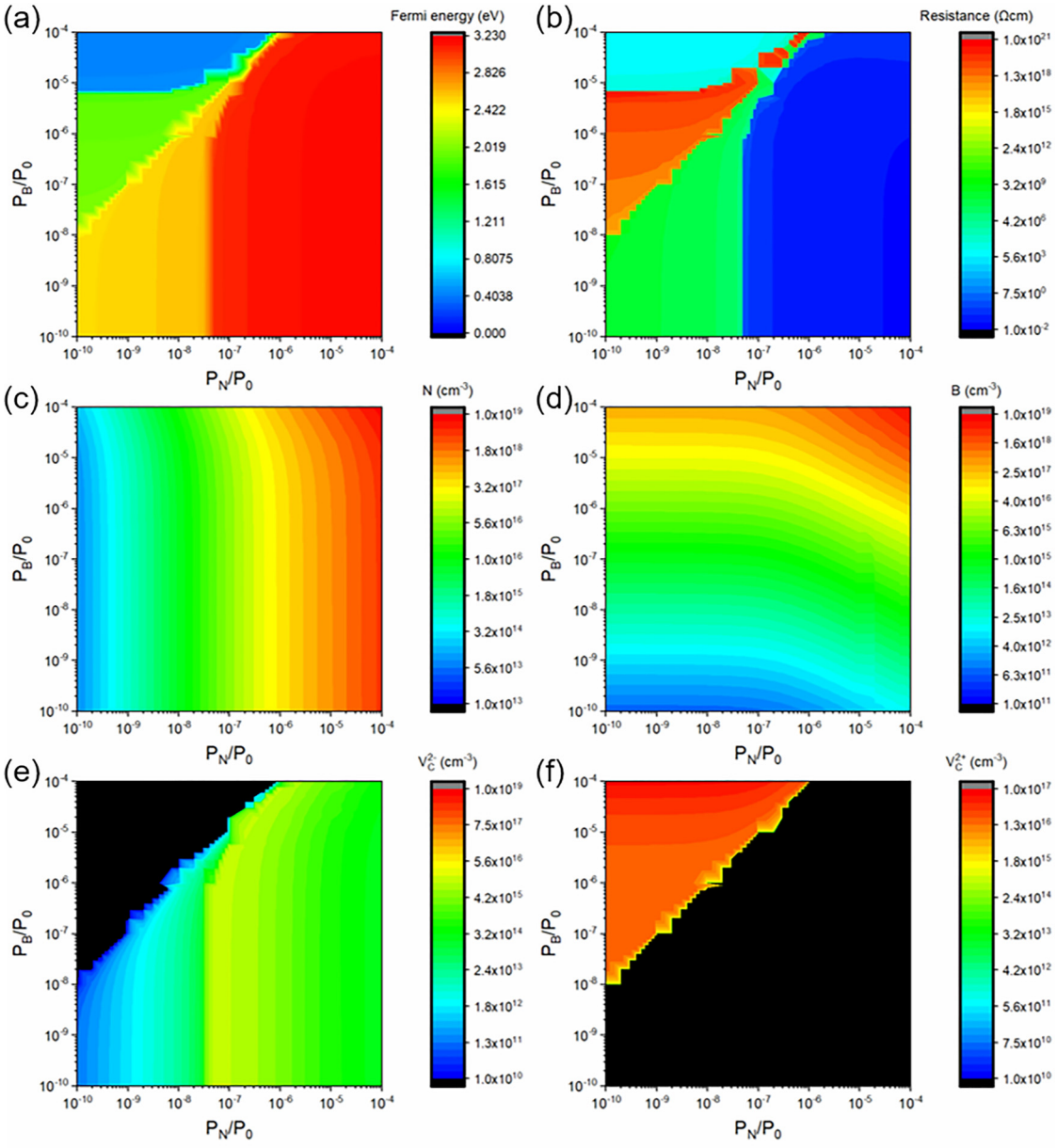

FIG. 3. (a) Fermi energy (E_F), (b) resistance, (c) N doping concentration, (d) B doping concentration, (e) V_C^{2-} concentration, and (f) V_C^{2+} concentration as functions of P_N/P_0 and P_B/P_0. Growth temperature is 2400 K, from which quenching reaches room temperature.

is the temperature, $P_{N/B}$ is the partial pressure of N/B, and P_0 is the total pressure during the growth of 4H-SiC. Due to the fact that $P_{N/B}$ is very low during growth, the effect of the change of $P_{N/B}$ on μ_{Si} and μ_C may be neglected. $\varepsilon(0/+)$ of N is calculated by Eq. (3). The calculated $\varepsilon(0/+)$ is 0.06 eV (0.12 eV) for the h (k) site. When Eqs. (2), (3), and (8) are combined, $\Delta H_f(N_C, 0)$ and $\Delta H_f(N_C, 1+)$ can be expressed as a function of P_N/P_0. Only one typical formation energy curve of N_C is shown in Fig. 2. B can occupy either Si or C sites of 4H-SiC. The calculated $\varepsilon(0/-)$ for B_{Si} is 0.30 eV, and the calculated $\varepsilon(0/-)$ for B_C is 0.42 eV. The formation energies of B_{Si} and B_C are also a function of P_B/P_0 (Fig. 2). The formation energy of N/B decreases with the increase of $P_{N/B}$.

It is commonly accepted that carbon vacancies (V_C) are the main intrinsic defects responsible for the semi-insulating behavior

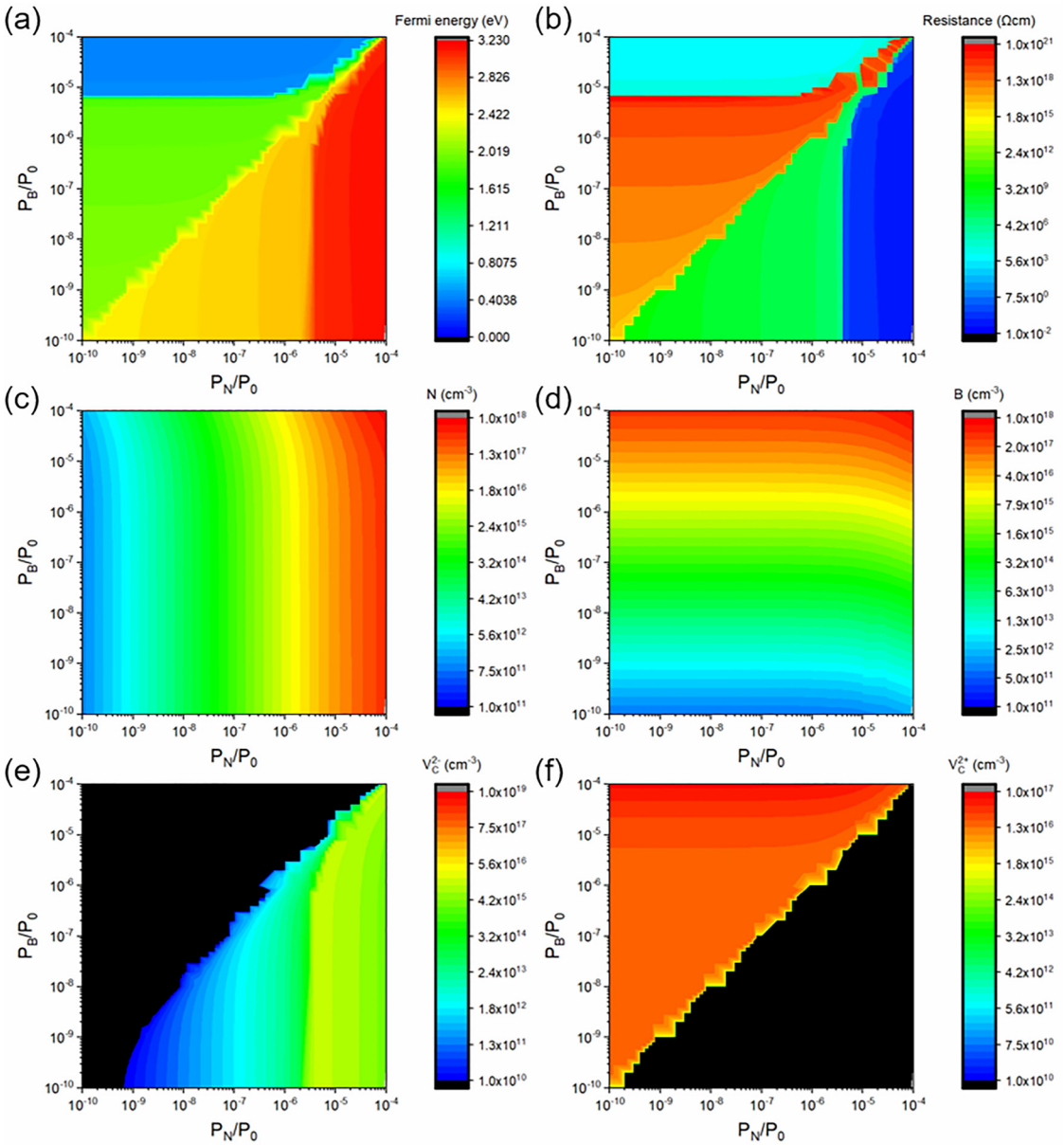

FIG. 4. (a) Fermi energy (E_F), (b) resistance, (c) N doping concentration, (d) B doping concentration, (e) V_C^{2-} concentration, and (f) V_C^{2+} concentration as functions of P_N/P_0 and P_B/P_0. Growth temperature is 2400 K, from which quenching reaches room temperature. The hydrogen is included during growth. Growth temperature is set to 2400 K, from which quenching reaches room temperature.

of PVT-grown 4H-SiC.[31–37] The formation energy of V_C is also calculated through Eqs. (1)–(3), as shown in Fig. 2. For the Si-rich limit, $\Delta H_f(V_C, 0)$ is about 4.42 eV. $\epsilon(0/2-)$ transition levels ($Z_{1/2}$) of V_C(h) (V_C at the h site) and V_C(k) (V_C at the k site) are located at $E_v + 2.60$ eV and $E_v + 2.67$ eV, respectively. The $\epsilon(2+/0)$ transition level (EH6/7) is located at $E_v + 1.84$ eV for V_C(h) and $E_v + 1.90$ eV for V_C(k), which agrees well with the experimental value.[35–37] Tuning the B and N doping concentration (DC_B and DC_N) relative to the concentration of V_C (DC_{V_C}) will have a substantial impact on the Fermi energy of 4H-SiC. When DC_N or $DC_B > DC_{V_C}$, N and B doping will make the Fermi level close to $\varepsilon(0/+)$ of N or $\varepsilon(0/-)$ of B (E_F^1 or E_F^5 in Fig. 2). When $DC_N - DC_B \leq DC_{V_C}$, the excess donors are compensated by V_C^{2-} and the Fermi energy is pinned at E_F^2. The addition of hydrogen could increase the formation energy of N. The Fermi energy is pinned at a deeper level ($E_F^{2'}$). When $DC_B - DC_N \leq DC_{V_C}$, the excess acceptors are compensated by V_C^{2+} and the Fermi energy is pinned at E_F^4. When N_N or N_B is close, the Fermi energy will be pinned at E_F^3.

By using a detailed balance theory,[21,22] we can obtain Fermi energies, resistance, the doping concentration of N/B, and V_C concentrations of 4H-SiC at a given partial pressure of P_N/P_0 and P_B/P_0, as shown in Figs. 3 and 4. In practice, quenching is often used to increase the concentration of intrinsic defects. Therefore, we also calculate the defect concentrations obtained with a typical growth temperature of 2400 K followed by quenching to room temperature by fixing the sum of defect concentrations and recalculating the density of the charged defects at room temperature.[38–40]

Figure 3 shows Fermi energy, resistance, N doping concentration, B doping concentration, V_C^{2-} concentration, and V_C^{2+} concentration as functions of P_N/P_0 and P_B/P_0 without the addition of hydrogen during the growth of 4H-SiC single crystals. Depending on Fig. 3(a), the distribution diagram of Fermi energy can be divided into four different regions: red region, yellow region, green region, and blue region. In the red region, when P_N/P_0 is higher than 3×10^{-8}, the Fermi energy is about $E_V + 3.19$ eV (close to E_F^1 in Fig. 2) and the resistance is in an order of 10^{-1} and $10^{-2}\,\Omega$ cm [Fig. 3(b)]. The doping concentration of N is higher than that of B [Figs. 3(c) and 3(d)]. The excess donors are not completely compensated by V_C^{2-} [Fig. 3(e)]. In the yellow region, the Fermi energy is about $E_V + 2.49$ eV (close to $Z_{1/2}$ of V_C), and the resistance is in the range of 10^6–$10^{12}\,\Omega$ cm [Fig. 3(b)]. In this region, $DC_N - DC_B \leq DC_{V_C}$, the excess donors are completely compensated by V_C^{2-} [Fig. 3(e)]. In the green region, the Fermi energy will be pinned at about $E_V + 1.89$ eV (close to EH6/7 of V_C), and the resistivity is higher than $10^{12}\,\Omega$ cm [Fig. 3(b)]. This is because $DC_B - DC_N \leq DC_{V_C}$ and the excess acceptors are completely compensated by V_C^{2+} [Fig. 3(f)]. As for the blue region, the doping concentration of B is higher than that of N and the excess acceptors are not completely compensated by V_C^{2-} [Fig. 3(e)]. The fermi energy is located at about $E_V + 0.40$ eV (close to E_F^1 in Fig. 2) and the resistivity is in the order of 10^3 and $10^4\,\Omega$ cm [Fig. 3(b)].

If hydrogen is added during the growth of 4H-SiC single crystals, HPSI 4H-SiC can be grown in a relatively high nitrogen partial pressure environment. The critical P_N/P_0 is 2×10^{-6}, as shown in Fig. 4. When P_N/P_0 is lower than 2×10^{-6}, the HPSI 4H-SiC can be grown. Assuming that the growth pressure P_0 is 100 Pa and hydrogen is not added during the growth, a HPSI 4H-SiC can be grown when the nitrogen partial pressure decreases to 3×10^{-6} Pa. When hydrogen is added during the growth, the nitrogen partial pressure lower than 2×10^{-4} Pa is sufficient to guarantee the growth of HPSI 4H-SiC. This indicates that the addition of hydrogen during growth could significantly mitigate the requirements of the growth system on vacuum and the purity of graphite parts and SiC source powders.

IV. CONCLUSIONS

In conclusion, we have investigated the effect of hydrogen on unintentional doping of N and B into 4H-SiC. It is found that the addition of hydrogen significantly mitigates N doping while hardly affecting B doping. When hydrogen is included in the growth of 4H-SiC, N may react with hydrogen to form stable NH_3. This decreases the chemical potential of N and increases the formation energy of N in 4H-SiC. Moreover, the adjustment of relative B and N doping concentrations has a substantial impact on the Fermi energy of HPSI 4H-SiC. When the doping concentration of N is higher than that of B, N interacts with carbon vacancies (V_C), pinning the Fermi energy at $Z_{1/2}$. The resistance is in the range of 10^6–$10^{12}\,\Omega$ cm. When the doping concentration of B is higher than that of N, the Fermi energy is pinned at EH6/7. The resistivity is high than $10^{12}\,\Omega$ cm.

ACKNOWLEDGMENTS

This work was supported by "Pioneer" and "Leading Goose" R&D Program of Zhejiang (Grant No. 2022C01021) and the Natural Science Foundation of China (Grant Nos. 91964107 and U20A20209). Partial support from the Natural Science Foundation of China for Innovative Research Groups (Grant No. 61721005) is acknowledged. The National Supercomputer Center in Tianjin is acknowledged for computational support.

AUTHOR DECLARATIONS

Conflict of Interest

The authors have no conflicts to disclose.

Author Contributions

Yuanchao Huang: Conceptualization (equal); Data curation (equal); Formal analysis (equal); Investigation (equal); Methodology (equal); Writing – original draft (equal); Writing – review & editing (equal). **Rong Wang:** Methodology (equal); Supervision (equal); Writing – review & editing (equal). **Naifu Zhang:** Conceptualization (equal); Investigation (equal); Writing – review & editing (equal). **Yiqiang Zhang:** Supervision (equal); Validation (equal); Writing – review & editing (equal). **Deren Yang:** Project administration (equal); Supervision (equal). **Xiaodong Pi:** Funding acquisition (equal); Investigation (equal); Methodology (equal); Project administration (equal); Supervision (equal); Validation (equal); Visualization (equal); Writing – review & editing (equal).

DATA AVAILABILITY

The data that support the findings of this study are available within the article.

REFERENCES

[1]T. Kimoto and J. A. Cooper, *Fundamentals of Silicon Carbide Technology: Growth, Characterization, Devices and Applications* (John Wiley & Sons, 2014).
[2]R. S. Pengelly, S. M. Wood, J. W. Milligan, S. T. Sheppard, and W. L. Pribble, IEEE Trans. Microwave Theory Tech. **60**, 1764 (2012).
[3]V. V. Buniatyan and V. M. Aroutiounian, J. Phys. D: Appl. Phys. **40**, 6355 (2007).
[4]A. R. Powell and L. B. Rowland, Proc. IEEE **90**, 942 (2002).
[5]X. Cai, C. Du, Z. Sun, R. Ye, H. Liu, Y. Zhang, X. Duan, and H. Lu, J. Semicond. **42**, 051801 (2021).
[6]R. Gaska, J. W. Yang, A. Osinsky, Q. Chen, M. A. Khan, A. O. Orlov, G. L. Snider, and M. S. Shur, Appl. Phys. Lett. **72**, 707 (1998).
[7]F. Fu, S. Deng, L. Wang, H. Liao, and J. Zhang, IEEE (SSL China: IFWS), 68 (2021).
[8]M. Bickermann, R. Weingärtner, and A. Winnacker, J. Cryst. Growth **254**, 390 (2003).
[9]H. Kaneko and T. Kimoto, Appl. Phys. Lett. **98**, 262106 (2011).
[10]M. A. Fanton, R. L. Cavalero, B. E. Weiland, R. G. Ray, D. W. Snyder, R. D. Gamble, and W. J. Everson, J. Cryst. Growth **287**, 363 (2006).
[11]J. R. Jenny, S. G. Müller, A. Powell, V. F. Tsvetkov, H. M. Hobgood, R. C. Glass, and C. H. Carter, J. Electron. Mater. **31**, 366 (2002).
[12]J. R. Jenny, D. P. Malta, S. G. Müller, A. R. Powell, V. F. Tsvetkov, H. M. Hobgood, and C. H. Carter, J. Electron. Mater. **32**, 432 (2003).
[13]D. P. Malta, J. R. Jenny, H. M. Hobgood, and V. F. Tsvetkov, U.S. patent 7,147,715 (Dec. 12, 2006).
[14]Y. M. Wang, R. S. Wei, L. Z. Wang, K. L. Mao, B. Li, and X. Dai, Mater. Sci. Forum **858**, 69 (2016).
[15]T. Furusho, S. K. Lilov, S. Ohshima, and S. Nishino, J. Cryst. Growth **237–239**, 1235 (2002).
[16]G. J. Fechko, Jr., J. R. Jenny, H. M. Hobgood, V. F. Tsvetkov, and C. H. Carter, Jr., U.S. patent 7,220,313 (May 22, 2007).
[17]J. R. Jenny, D. P. Malta, H. M. Hobgood, S. Mueller, and V. F. Tsvetkov, U.S. patent 6,814,801 (Nov. 9, 2004).
[18]M. A. Fanton, Q. Li, A. Y. Polyakov, M. Skowronski, R. Cavalero, and R. Ray, J. Cryst. Growth **287**, 339 (2006).
[19]Q. Li, A. Y. Polyakov, M. Skowronski, M. A. Fanton, R. C. Cavalero, R. G. Ray, and B. E. Weiland, Appl. Phys. Lett. **86**, 202102 (2005).
[20]G. Kresse and J. Hafner, Phys. Rev. B **47**, 558 (1993).
[21]S. H. Wei, Comput. Mater. Sci. **30**, 337 (2004).
[22]Y. Huang, R. Wang, Y. Zhang, D. Yang, and X. Pi, Chin. Phys. B **31**, 046104 (2022).
[23]A. Jain, S. P. Ong, G. Hautier, W. Chen, W. D. Richards, S. Dacek, S. Cholia, D. Gunter, D. Skinner, G. Ceder, and K. A. Persson, APL Mater. **1**, 011002 (2013).
[24]E. Scalise, A. Marzegalli, F. Montalenti, and L. Miglio, Phys. Rev. Appl. **12**, 021002 (2019).
[25]C. F. Cline, J. Electrochem. Soc. **106**, 322 (1959).
[26]I. Tomaszkiewicz, J. Therm. Anal. Calorim. **65**, 425 (2001).
[27]X. Luo, S. B. Zhang, and S. H. Wei, Phys. Rev. Lett. **90**, 026103 (2003).
[28]S. B. Zhang and S. H. Wei, Phys. Rev. Lett. **86**, 1789 (2001).
[29]C. Cavallotti, F. Rossi, S. Ravasio, and M. Masi, Ind. Eng. Chem. Res. **53**, 9076 (2014).
[30]P. Atkins and J. De Paula, *Physical Chemistry* (Macmillan, 2002).
[31]N. T. Son, B. Magnusson, Z. Zolnai, A. Ellison, and E. Janzén, Mater. Sci. Forum **457–460**, 437 (2004).
[32]N. T. Son, P. Carlsson, A. Gällström, B. Magnusson, and E. Janzén, Physica B **401,402**, 67 (2007).
[33]G. Alfieri, T. Kimoto, and G. Pensl, Mater. Sci. Forum **645–648**, 455 (2010).
[34]G. Alfieri, L. Knoll, L. Kranz, and V. Sundaramoorthy, J. Appl. Phys. **123**, 175304 (2018).
[35]N. T. Son, X. T. Trinh, L. S. Løvlie, B. G. Svensson, K. Kawahara, J. Suda, and E. Janzén, Phys. Rev. Lett. **109**, 187603 (2012).
[36]I. Capan, T. Brodar, Z. Pastuović, R. Siegele, T. Ohshima, S. I. Sato, and K. Demmouche, J. Appl. Phys. **123**, 161597 (2018).
[37]X. Cai, Y. Yang, H. X. Deng, and S. H. Wei, Phys. Rev. Mater. **5**, 064604 (2021).
[38]J. H. Yang, J. S. Park, J. Kang, W. Metzger, T. Barnes, and S. H. Wei, Phys. Rev. B **90**, 245202 (2014).
[39]J. Ma, S. H. Wei, T. A. Gessert, and K. K. Chin, Phys. Rev. B **83**, 245207 (2011).
[40]Y. Huang, R. Wang, Y. Zhang, D. Yang, and X. Pi, J. Appl. Phys. **131**, 185703 (2022).